12.263   **ICING HAZARD DETECTION WITH NEXRAD IHL**

Robert G. Hallowell *, Michael F. Donovan, David J. Smalley, Betty J. Bennett

MIT Lincoln Laboratory

1. INTRODUCTION

In-flight aircraft icing is a well-known problem for aviation. Icing conditions typically occur when the aircraft comes in contact with supercooled liquid water (SLW) in the atmosphere – the unstable water perturbed by the aircraft readily transforms to ice attaching to all parts of the aircraft. This build-up of ice on the skin of the aircraft and in particular on the wings causes increased drag resulting in a loss of lift to the aircraft. While large aircraft often have mitigation measures for airframe icing, air taxi and general aviation aircraft are both less likely to have sufficient mitigation measures and are more likely to fly at levels conducive to icing. Not surprisingly, a review of the past 10 years of fatal accidents due to icing shows that over 90% of these incidents are in non-Part 121 aircraft (NTSB 2013).

Supercooled liquid water droplets range in size and density. The smallest droplet sizes make direct measurement of SLW droplets by remote sensing beyond the scope of current operational radar systems. However, drizzle drops and large supercooled water drops are detectable, although they are often mixed with other forms of hydrometeors making detection challenging. These types of droplets are important in that they present a clear ice hazard. By utilizing the upgraded dual-polarization (herein referred to as dual-pol) Next Generation Weather Radar

(NEXRAD) data and combining it with thermodynamic information from Numerical Weather Prediction (NWP) model data, it is possible to identify high probability regions of icing. MIT Lincoln Laboratory (MITLL) has been funded by the Federal Aviation Administration (FAA) to leverage and extend the existing research on radar-based icing detection in order to implement an icing detection product in the NEXRAD Open Radar Product Generator (ORPG) system (Ganger 2002; Smalley 2002). This paper discusses a baseline Icing Hazard Levels (IHL) product to be available in Build 14 of NEXRAD, and the supporting algorithms that should yield further improvements in NEXRAD based detection and estimation of icing regions.

2. BACKGROUND

There are a number of aviation products that attempt to address the in-flight icing hazard. These include: pilot reports (PIREPs) from aircraft that have been experiencing icing, non-convective Significant Meteorological Information (SIGMET) and Airmen's Meteorological Information (AIRMET) notices provided by the National Weather Service (NWS), and the Current and Forecast Icing Potential (CIP/FIP) products provided through the NWS Aviation Weather Center's (AWC) Aviation Digital Data Service (ADDS).

PIREPs provide direct observations of icing conditions, including type, severity and affected flight levels and are obviously valuable for pilots that are following in the path of the same aircraft. However, icing reports are not mandated and therefore the reporting of events is typically sparse. In addition, because the reports are either reported over the radio or downloaded via the Aircraft Communications Addressing and

Reporting System (ACARS), and the process requires a manual observation, the reporting is frequently delayed and the specific information can be incorrect or outdated (Bernstein 2007). Nevertheless, these reports are valuable because they currently provide the only routine means for verification of in-flight icing conditions (FAA 2013a).

The NWS non-convective SIGMET/AIRMET notices provide current and forecasted conditions tailored to pilots and, in the case of icing, are created using available forecast information (PIREPs, radar, satellite, and NWP models). An AIRMET is used for moderate and widespread icing conditions while an icing SIGMET is issued for specific areas of severe icing. Many of these reports are triggered by pilot reports and while the meteorologist will look for verifying conditions and forecasts, the accuracy can be subject to the same limitations of the initial pilot report (FAA 2013b).

Currently, the most comprehensive icing potential forecast is given by the CIP/FIP products. CIP utilizes a combination of observations from satellite, surface stations, radar, PIREPs, lightning sensors, and NWP model output to create a gridded, hourly diagnosis of aircraft icing potential by flight level. Forecasted icing conditions utilize NWP model fields as surrogates for detection criteria (Wolff et al. 2012; Adriaansen et al. 2012).

3. DUAL-POLARIZATION NEXRAD

While the existing icing products, and in particular CIP/FIP, provide good coverage and quality for the potential of icing conditions, the advent of dual-pol NEXRAD creates an opportunity to improve icing detection capabilities within the radar coverage domain at a high temporal and spatial resolution. As can be seen from Figure 1, NEXRAD coverage across the United States for icing up to ten thousand feet above ground level (AGL) is quite good, except in the Western CONUS where mountain barriers and more limited siting options yield some significant gaps. At higher altitude levels the radar coverage is extended; however, optimal icing coverage requires multiple radar tilts at varied altitudes.
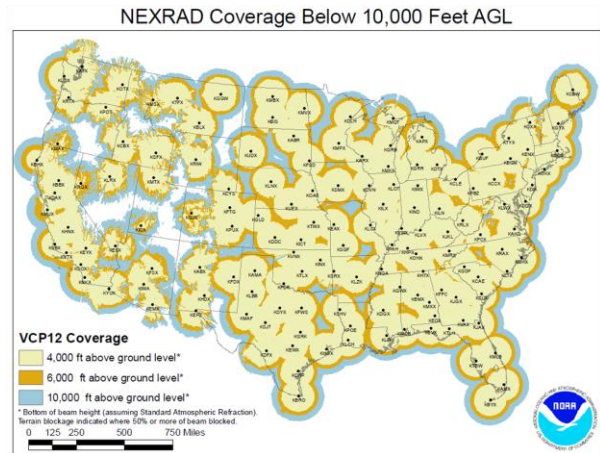

Fig. 1. NEXRAD coverage map of the continental United States (NOAA) below 10,000 feet AGL.

So, why is it important to develop a dedicated icing product within the NEXRAD system? First, despite gaps in coverage, more than 80% of the country can be fully scanned for icing by NEXRAD making it far superior to PIREP observations in terms of coverage. In addition, most icing PIREPs occur near frontal systems that are likely to be associated with precipitation making NEXRAD a great tool for detection. Third, while level II products from NEXRAD could be combined outside the NEXRAD system, some details, such as the relative weighting of hydrometeor classification categories, are not available to external systems and these details yield significant clues as to the probability of icing conditions. Next, a highly accurate icing product derived from detailed radar data and other peripheral information available within NEXRAD would create a firm basis for interpolated fields of icing by providing high quality waypoints for icing conditions. And, finally, this radar-based product could yield improvements in multi-sensor, multi-model interest fields of icing detections and forecasts outside of NEXRAD.

4. NEXRAD ALGORITHM SUPPORT FOR IHL

The goal of the NEXRAD Icing Hazard Levels (IHL) algorithm is to create a product that delineates the top and bottom of regions where icing is likely to be occurring based on information available within the NEXRAD ORPG system. There are currently no direct icing products

available from the initial suite of NEXRAD dual-pol algorithms; however, there are several products that are related to icing activity. They are: the Hydrometeor Classification Algorithm (HCA), the Melting Layer Detection Algorithm (MLDA), and the internal NWP model data processing capability. Each of the icing-related products above yield clues as to the icing environment, but in order to create a direct icing product the data must be combined and, in some cases, modified to provide improved icing detection capabilities. Figure 2 illustrates the interdependencies of each of the existing NEXRAD algorithms; products and data are in blue while the new IHL algorithms and data are in brown.
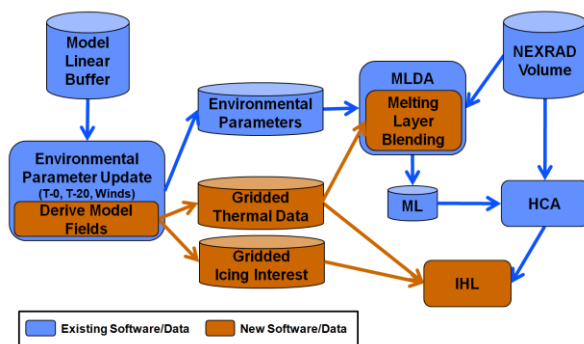

Fig. 2. Flowchart showing the interdependencies among NEXRAD algorithm and data components that are essential to the development of the IHL algorithm. Cylinders represent data stores and rectangles represent algorithm modules. The blue and brown components represent existing and new software and data to be deployed with Build 14, respectively.

Each of the icing-related products is used as a component of the new IHL algorithm. Therefore, it is useful to start with an overview of these products and identify the challenges and solutions that were developed for each product/algorithm to make them suitable for IHL.

4.1 *Hydrometeor Classification Algorithm*

The HCA was specifically developed for the polarimetric NEXRADs (Park et al. 2009) and is designed to identify the predominant category of scatterers within a radar resolution volume. The

algorithm utilizes thresholds in various radar parameters and the location relative to the melting layer (ML) to determine what categories are allowable within a certain range bin. This thresholding reduces the possibility of incorrectly identifying ice (liquid) categories in regions well below (above) the ML. Figure 3 shows the categories that are allowed (green) and not allowed (grey) within the HCA relative to different ML combinations. There are eight precipitation categories of hydrometeor classification (heavy rain, big drops, ice crystals, light/moderate rain, wet snow, dry snow, rain/hail mix, and graupel), two categories of contaminants (ground clutter and biological), and two categories of unclassified (no echo and unknown). While verification of rain/hail and heavy rain are fairly straightforward based on surface observations, other upper-level categories are more challenging to verify. Therefore, caution must be used in creating derived products based solely on the HCA category.

Fig. 3. Chart illustrating the hydrometeor categories within the HCA and their relationship to the probability of icing relative to a single ML. The green and grey filled boxes represent the category designations whose location relative to the ML are allowed or not allowed by the algorithm, respectively. The sorting of categories within the chart depicts the increasing likelihood of the presence of SLW when moving from left to right and bottom to top.

The first version of the HCA, developed by the National Severe Storms Laboratory (NSSL), was designed to work in summer environments where large scale convective activity was the primary focus (Heinselman and Ryzhkov 2006). While significant improvements have been made to the algorithm, there remain shortcomings to the

existing algorithm when the focus is large scale winter storms and complicated thermodynamic profiles (Elmore, 2011). In particular, SLW is currently not a defined class; the operational limits of the radar make direct detection very challenging. However, modeling theory and experimental research show that SLW is generally co-located in regions where other hydrometeors are the predominant feature. The categories in Figure 3 have been sorted from left to right and bottom to top based on the possibility that SLW is co-located with a particular category. By definition, a category such as graupel or snow pellets infers the presence of supercooled droplets (American Meteorological Society 2013) because SLW is responsible for the rime ice that encapsulates ice crystals. Based on research aircraft observations, other categories such as dry snow tend to cover a wide variety of ice crystal conditions, and in some cases SLW is co-located within these dry snow regions (Smalley 2013). The ice crystal category indicates a decreasing likelihood of SLW but it can potentially pose an aviation hazard as there have been numerous incidences where ice crystals ingested into aircraft engines resulted in the rapid buildup of ice in the engine exhaust (Haggerty 2012). The remaining precipitation hydrometeor categories consisting of light/moderate rain and wet snow are generally icing threats only in regions where HCA does not allow the category (grey boxes). These are areas where future research may prove useful in extracting the presence of SLW mixing. While not sufficient to declare the existence of SLW and/or icing, the HCA categories provide an initial breakdown of icing potential.

4.2 *Melting Layer Detection Algorithm*

The NEXRAD MLDA produces a radial by radial estimate of the top and bottom of the ML by searching for polarimetric signatures of melting snow (Giangrade et al. 2008). If sufficient evidence of melting snow is found, the algorithm attempts to determine the location of the radar "bright band" – a range of elevated radar responses caused by the mix of water and ice as the atmosphere transitions from above to below freezing when moving out in range along a radial.

In MLDA, elevated and nearly co-located regions of reflectivity (Z), cross-correlation coefficient (CC), and differential reflectivity (ZDR) all indicate evidence of wet snow and contribute weight for the elevation angle where it was detected. The weights for each elevation angle are then summed to see if sufficient evidence exists for a bright band. Radials with enough interest yield high and low beam height calculations to estimate the top and bottom of the ML. Figure 4 shows evidence of a typical single crossing ML signature within three dual-pol products for a 4.3° plan position indicator (PPI) tilt, with black lines representing the radar based estimate of the ML top (far out in range) and bottom (close in range).
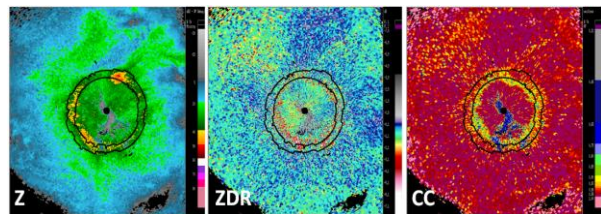

Fig. 4. Example of a typical single ML signature found in the Z (left), ZDR (middle), and CC (right) products for a 4.3° elevation angle. The black contours represent the top and bottom of the ML product detected by the MLDA.

In cases where no radar bright band signature can be found, the algorithm examines the available NWP model data from the model grid point closest to the radar location and computes the interpolated freezing level height among all pressure levels available in the model column. The height of the 0°C crossing value is then applied to all radials. If no model data is available, the ML ultimately defaults to an average freezing level height parameter value for the particular NEXRAD location.

The MLDA performs well and has shown good agreement with radiosonde observations and model temperature profiles for stratiform precipitation events in which there is substantial detection of wet snow and the ML is above 1 km AGL. However, in complicated cases involving multiple crossings over short altitude distances, the bright band signature is often broad and ill-defined, and, in the case of ground temperatures

at or near freezing, non-existent. In these cases the model data can serve as a default but the accuracy of ML detection over the entire radar domain is limited to identifying a single crossing at the radar site. For these reasons, the NWS Warning Decision Training Branch (WDTB) has recommended that the NWS office should interactively set their own freezing height based on available data. These instances are commonly observed during cold season events in which there are synoptic scale cold and warm frontal passages creating a transient sloping ML.

Figure 5 is an illustration of the dual-pol CC product for a 4.0° PPI tilt and an example of how the MLDA handles a strong cold front that approached the Wichita, Kansas NEXRAD (KICT) from the north with temperatures below freezing in its wake. The atmosphere well ahead of the front to the southeast is above freezing at the surface with a single elevated 0°C crossing at approximately 3.1 km AGL. Black contour lines denote the ML top (far out in range) and bottom (close in range) product produced in the current MLDA. The radar-diagnosed ML regions indicated as RD between the arrows, match nicely with the visible bright band to the southeast and are used to calculate an average ML height for all the radials noted in the RA regions where there is little or no evidence of a bright band. The result is an accurate ML to the southeast but an estimate to the north that far exceeds the much lower freezing level noted in the model and where surface temperatures are close to freezing.

In order to address this problem, MITLL expanded the use of the NWP model data in order to merge it with radar-based radials when there is limited or non-existent evidence of a bright band feature. The use of model data in MLDA is explained further below.

4.3 *Environmental Model Data*

Environmental model data are updated into each NEXRAD ORPG system on an hourly basis through the Advanced Weather Interactive Processing System (AWIPS). AWIPS subsamples the full domain National Center for Environmental

Prediction (NCEP) Rapid Refresh (RAP) model into a smaller grid centered at the radar site with coverage extending over the entire radar scanning domain. The three dimensional model data consists of either the one or two hour forecast of temperature, relative humidity, geopotential height and the u and v wind components for each constant pressure level. Depending on the radar site configuration settings, the horizontal resolution of the model received can either be 13 or 40 km. Of importance to icing hazard detection, the freezing level height is computed by locating the pressure level where the temperature first goes above 0°C in a top-down search order and the height is interpolated between the two levels that bound the crossing. As mentioned in the previous section, the estimation is only performed for the model grid point nearest the radar site and subsequently gets updated into the system adaptation data to be available for use by the MLDA.
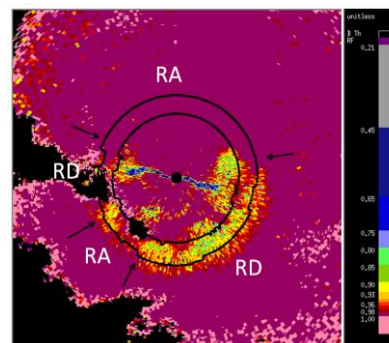

Fig. 5. Dual-pol CC product at the 4.0° PPI tilt for a cold front that approaches the KICT NEXRAD from the north. The black contour lines denote the ML top and bottom product produced in the current MLDA. Regions between the arrows denote locations of the radar diagnosed (RD) and radar averaged (RA) ML where there is sufficient or weak to no evidence of a bright band signature in the radar data, respectively.

In order to utilize the model data more effectively within MLDA, MITLL expanded the processing within the ORPG to allow full access to the model grid. This new set of library calls allows for the creation of two data buffers, named the Thermal Grid and Icing Interest buffer. The Thermal Grid buffer summarizes a number of melting layer

related data fields computed among all pressure levels of the model for each model grid point. Table 1 shows the contents of this buffer listed on the right. The third field listed contains a grid of the number of 0ºC crossings computed within each column of model data. A bin with a "1" is the common value indicating a single crossing of the freezing level. A "0" would be indicative of a case where the temperature at the surface is below freezing and there are no warm layers above. A number between 2 and 5 indicates a more complicated thermodynamic structure with multiple 0ºC crossings (inversions, turbulent frontal passages, or an atmosphere where the temperature fluctuates around 0ºC at multiple layers). Grid fields 4-9 within the buffer contain the interpolated heights for each crossing point found. An example of the type of temperature profile encountered for each number of crossings and a count of the number of warm and cold layers found are illustrated in columns 1-4 of Table 1. An expanded illustration of temperature profiles for a single and double crossing of the 0°C threshold are provided in Figure 6 on the left, and the model gridded representation of the geopotential height for each 0°C crossing and a grid of the crossings count are shown on the right.

Table 1. Table illustrating the contents of the newly created Thermal Grid buffer available within the NEXRAD ORPG. A list of the 20 fields computed for each model grid point among all pressure levels is shown on the right. Columns 2-4 in the table represent the number of 0°C crossings and the number of warm and cold layers found, respectively, among the temperature vs. height profile scenarios shown in the first column while descending in altitude toward the surface.

Profile Type	# 0°C crossings	# warm layers	# cold layers
	0	0	0
	1	1	0
	2	1	1
	3	2	1
	4	2	2
	5	3	2

Thermal Grid
Levels - 20
Grid Dimensions - ~61 x 61

Grid order:
1 – range of grid point
2 – azimuth of grid point
3 – num 0° C crossings
4 – height of 1st 0° C crossing
5 – height of 2nd 0° C crossing
6 – height of 3rd 0° C crossing
7 – height of 4th 0° C crossing
8 – height of 5th 0° C crossing
9 – height of 6th 0° C crossing
10 – height of -10° C (ZDR BB)
11 – height of -16° C (ZDR BB)
12 – height of -20° C
13 – max temp warm layer 1
14 – max temp warm layer 2
15 – max temp warm layer 3
16 – min temp cold layer 1
17 – min temp cold layer 2
18 – spare
19 – spare
20 – spare

The buffer is set up to store multiple height grids of each crossing point and the maximum and minimum temperature within each warm or cold layer, respectively. For the initial version of IHL, however, we focus on the altitude of the highest 0ºC crossing level (field 4 in Table 1) because this value approximately represents the top of the ML computed by the MLDA from radar data alone.
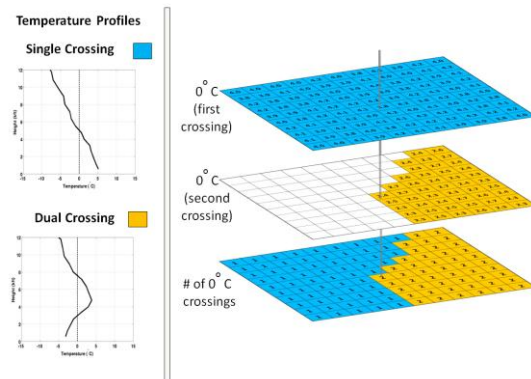
Fig. 6. Illustration showing a gridded representation of the heights and number of 0°C crossings computed from the NWP model for all grid points. Each blue and gold colored grid bin represents the temperature profile scenario shown on the left. Grid bin values within the two upper grids are example height altitudes of each 0°C crossing and the bottom grid is a count of the number of crossings computed in each model column.

Figure 2 shows the modified flow of the MLDA algorithm to take advantage of the model based estimates. Prior to blending model data with the radar-based ML, the latitude-longitude location of

each model grid point is converted to a range-azimuth bin in polar coordinates relative to the radar site. A model-simulated radial-by-radial ML is then computed by averaging the top level crossing height over a range of 0-150 km and +/- 10 degrees in azimuth. These range-azimuth window parameters were chosen after comparing summertime radar-based MLDA calculations with model-based ML values and varying the extent of the window size until they matched. Next, we calculate the radar-based ML the same way as it has always been done in the MLDA. Finally, the model-radar blending of the ML is performed according to the following rules:

- Valid radar-based ML radials have highest priority
- Small gaps in radar-based radials that have weak evidence of a bright band are filled with interpolated values of neighboring valid radials (as opposed to using the average over all valid radar radials)
- Larger gaps in radar-based radials that have weak evidence of a bright band are weight averaged (based on the level of "bright band" interest for the radial) with the model-based radials
- Model-based radials are used to replace radar-based radials that have no evidence of a bright band

Figure 7 is the companion to Figure 5 but shows the results of the model-radar merging in the modified MLDA. Note that the radar based radials to the southeast are the same as before, but the model data fills in to the north with the lower altitude freezing level depicted in the model. The improved MLDA is critical because so many HCA categories key off where the radar is scanning in relation to the ML (Figure 3).

5. ICING HAZARD LEVELS ALGORITHM

The goal of the IHL algorithm is to output a flat-earth polar representation of icing hazard regions. This process begins by identifying the HCA categories shown in Figure 3 that have a direct

relationship to icing based on hydrometeor classification alone. The two categories where icing is likely to be occurring simultaneously are the graupel and rain/hail categories. These are categories where extensive validation has been done based on surface evidence. Hail hazards are explicitly handled by NWS-issued Severe Thunderstorm Warnings and a new MITLL algorithm similar to IHL called Hail Hazard Layer (HHL) which identifies the top and bottom altitude of hail regions. In addition, hail is generally confined to convective events and not the wide-scale icing conditions that IHL is focused on. Graupel, on the other hand, is a category of precipitation that occurs not only in convective but also stratiform icing conditions. Therefore, the first step in the IHL algorithm is to search for the graupel class among each range bin in all tilts of the radar volume. Once this is complete, the highest and lowest altitudes of the tilts (total beam width included) containing graupel are calculated for each bin, much like NEXRAD currently maps vertically integrated liquid water (VIL) to a single range bin projected onto a 0° PPI tilt. The computed altitudes then define the IHL top and bottom products of the icing layer, respectively. Graupel that is found in a single tilt will have a top and bottom altitude mapped to the range bin for that tilt.
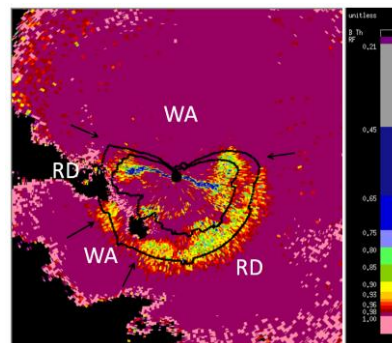

Fig. 7. Illustration as in Figure 5 showing results of the model-radar merging in the MLDA. Regions between the arrows denote locations of radar diagnosed (RD) and model-radar weighted average (WA) ML where there is sufficient or weak evidence of a bright band signature in the radar data, respectively.

Since graupel represents a transition category between frozen and liquid precipitation, graupel will tend to be located at the bottom of a column of icing. The image on the left in Figure 8 shows an example of graupel class placement within a 1.5° hydrometeor classification PPI tilt. The corresponding cross section through the radar volume along the dashed line in the PPI image is displayed on the right. Graupel (dark pink) is located in a thin band around the 0°C line (red contour line) shown in the cross section image. Dry snow is located above the graupel and rain and wet snow below it. The graupel gives the IHL a high quality representation of the bottom of the icing area.
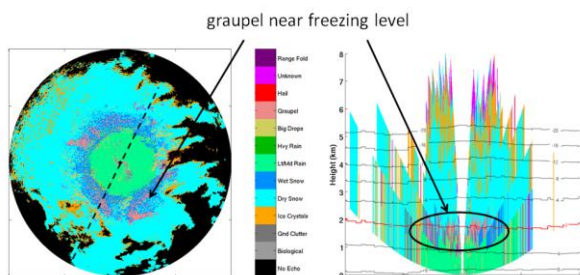

graupel near freezing level

Fig. 8. An example of the hydrometeor classification product for a 1.5° PPI tilt on the left, and a corresponding cross section through the radar volume along the dashed line in the PPI image on the right. Horizontal lines in the cross section image are model forecast temperature contours valid for the radar volume time. Note the graupel class, shown as dark pink, is located near the freezing level (red contour) and represents the bottom of the icing area.

Icing PIREPs are often located at altitudes higher than the regions of identified graupel in areas commonly classified as dry snow or ice crystals in the HCA. By utilizing techniques developed by the National Center for Atmospheric Research (NCAR) for creation of the CIP fields (Bernstein et al. 2005), NWP model data can be used to identify regions where atmospheric conditions may be conducive to icing and to augment IHL detections based on graupel alone.

CIP utilizes fuzzy scoring functions to produce interest maps based on various criteria (temperature, relative humidity, vertical motion,

satellite imagery, etc). The RAP model ingested into the NEXRAD ORPG system has a limited set of variables for use, and as such, IHL is restricted to using interest fields based on temperature and relative humidity. Figure 9 shows the scoring functions used by the NCAR CIP algorithm for temperature and relative humidity. The interest is based on a scale of 0 to 1, with 1 being high interest for icing. Interest is maximized under high relative humidity conditions and temperatures that are generally between -12 and -3°C. A model icing interest (MII) field is created by multiplying the two interest fields together and is included in the Icing Interest buffer mentioned in Section 4.3. Figure 10 shows an example of a MII cross section valid for the HCA PPI tilt and along the dashed line shown in Figure 8. Note that the region of high icing interest is above the layer where graupel is being detected.
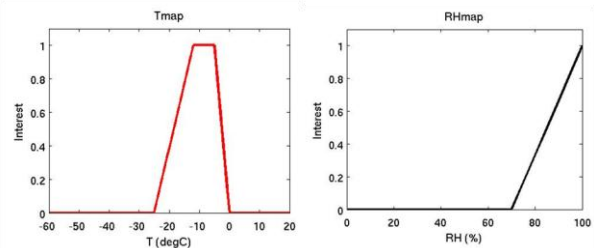

Fig. 9. Scoring functions for icing interest based on model temperature (left) and relative humidity (right).
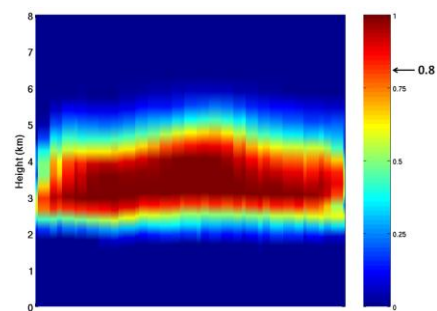

Fig. 10. Cross section of the MII field valid for the radar volume shown in Figure 8 along the dashed line displayed in the left image of that figure. Note the high icing interest region (≥ 0.8) is above the altitude where graupel is detected in the cross section image in Figure 8.

To expand IHL detections, the MII field is used only to extend the icing regionally above an

already identified region of graupel. An interest threshold value of 0.8 is utilized to find high interest regions, meaning on average interest from temperature and relative humidity are both in excess of 0.9. The MII threshold value chosen is discussed further in Section 6. Figure 11 illustrates the utility of the model extension by showing a cross section of the graupel-only based IHL detection (top and bottom) relative to the vertical extension based on the high MII regions shown in Figure 10.
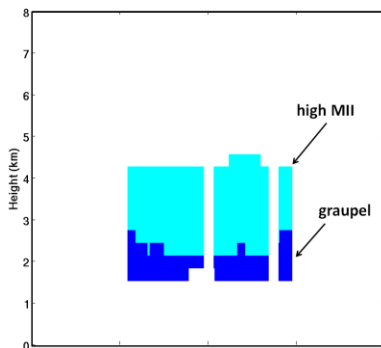

Fig. 11. Cross section showing the IHL detection based on graupel-only (dark blue) relative to the enhancement regions based on model data (cyan) for the radar volume and MII fields shown in Figs. 8 and 10, respectively.

The NEXRAD IHL product provides the top and bottom altitudes (vertical extent) of icing throughout each radar volume. The product reports the icing altitudes at a vertical resolution of 1000 feet referenced to mean sea level (MSL) on a 1° by 1 km polar grid to a range of 300 km. The altitude data range is >0 to ≤70 kft and the products are updated once per volume scan time. The icing altitude top and bottom products are each accompanied with an indexed severity and confidence component. Severity relates to the intensity of icing and confidence relates to the assessed quality of the graupel classification plus additional corroborating evidence. For the initial IHL algorithm, these component products are not computed but are defined as part of the product structure so that they may be readily available for future use. Figure 12 is an example of the IHL top and bottom polar grid products computed for the radar volume and MII field examples shown in Figs. 8, 10, and 11.
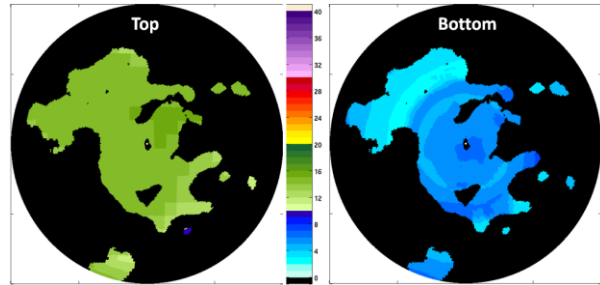

Fig. 12. IHL Top (left) and Bottom (right) polar grid products for the example case shown in Figs. 8, 10, and 11. Product units shown are in kft MSL.

6. VERIFICATION

There are several verification methods that are being examined in parallel: ground observations, PIREPs, and in situ aircraft measurements. The insights gathered from these methods are being used to: (1) study and characterize the relationship of the dual-pol signatures found in icing and non-icing environments, (2) how well the initial version of IHL performs and (3) determine new techniques and modifications to extend IHL into regions currently not being addressed (i.e., above the ML where a majority of the icing reports are located and beneath the ML where refreezing and regeneration of SLW can occur due to multiple freezing level scenarios).

During the 2009-10 and 2010-11 winter seasons, MITLL partnered with Valparaiso University to combine the operations of their C-band dual-pol radar with student ground observations and numerous atmospheric balloon soundings (Smalley 2011). These exercises yielded interesting findings in the thermal and moisture profiles associated with synoptic scale and lake effect storms and the discovery of Category "A" and "B" (Williams 2011) radar signatures observed in several events. These regions are associated with higher and lower icing potential regions, respectively. Similarly, surface classification observations of crystal type and whether the crystals were rimed or not were recorded this past winter season for several events in eastern Massachusetts. These recordings will be compared with the HCA product and the radar

signatures associated with riming/no riming conditions.

During IHL development, icing PIREP data were used to examine the utility of extending the graupel-only IHL with model data. For the initial study, a set of 22 PIREP cases from February 2012, where icing was located within or above graupel regions, were investigated. Among the cases, 73% of the reports were located above the HCA graupel detections. Adjustments to the IHL MII parameter were made until the highest percent of overlap between the PIREP altitude and the vertical extent of the IHL product was achieved. 27% of the PIREP cases remained above the graupel detections with the MII parameter set to 0.8. A larger scale analysis of PIREP comparisons is now being performed to tune the parameters within IHL and to explore the characteristics of the dual polarimetric products and other HCA category regions collocated with icing PIREPs.

Finally, a companion paper in this conference (Smalley 2013) discusses an FAA NEXRAD program supported partnership between MITLL and the Canadian National Research Council (CNRC) to conduct four in-flight icing missions within the Cleveland, OH and Buffalo, NY NEXRAD dual-pol coverage areas for verification and validation of hydrometeors and identification of potential icing hazards. Each flight presented a diverse weather system from which to collect observations. MITLL monitored the progression of each flight in real time and provided assistance in guiding the aircraft into interesting features observed within the NEXRAD radar data. The in situ aircraft measurements will be used to verify MLDA, IHL and HCA.

7. SUMMARY AND CONCLUSIONS

For the first time, an icing detection product will be available in the NEXRAD suite of algorithms as part of the next software deployment release (Build 14) scheduled for early 2014. The initial version of the IHL algorithm will identify the altitude top and bottom of an icing layer by deriving the radar beam altitudes where graupel was observed in the HCA. The top altitude can be further extended if significant MII is located above the height of the graupel. The icing product is created once per radar volume scan time and contains severity and confidence components (reserved for future use) which will accompany the altitude top and bottom products. To improve the fidelity of hydrometeor classification, updates to the NWP model ingest software create derived model fields over the entire radar coverage area. Blending techniques were also added to the MLDA that make use of these grids to improve ML detection of non-uniform freezing levels and weak bright-band signature scenarios.

The initial version of the IHL algorithm is limited in scope to regions where graupel is detected at some level of the atmosphere. As a result, there are caveats to this initial version that need to be mentioned. For one, icing detection is limited to the sensitivity limits of the radar. Icing is commonly observed in low signal environments for which the weight thresholding in the HCA does not allow graupel as a class and thus it will not be detected by the IHL algorithm. The inclusion of model information over the entire radar domain and blending with radar diagnoses of the ML in the MLDA have shown better performance, but there are instances in which the model information doesn't accurately capture the state of the environment. These situations ultimately impact the quality and accuracy of the HCA and IHL products. Despite improved performance, the MLDA is currently only designed to detect a single ML and can't support detection of low level refreezing layers and subsequent regeneration of SLW. Furthermore, the resolution of the model data received at the ORPG radar site (13 or 40 km), the volume coverage pattern (VCP) in operation, or changing from one VCP to another can all impact the accuracy and continuity of icing detection. Finally, since the vertical extent of the icing detection is controlled by radar beam thickness and the number of tilts where graupel was detected with possible model enhancement, the vertical extent of the icing may overestimate the existence of SLW. The IHL products, as they stand now, are not meant to be stand-alone but rather as ancillary information that would represent

value added to weather forecasters and external automated systems.

Despite these shortcomings, the initial IHL algorithm has shown the ability to detect icing for a subset of known icing scenarios. In addition, the deployment within the ORPG infrastructure serves as a basis from which additional modules and techniques will be developed. These new features will include: freezing drizzle aloft, multi-level freezing levels, mixed phased components. In addition, in-situ verification has already provided new insights that may provide additional leveraging of radar-based observations. All of these enhancements will yield expanded coverage and performance for IHL in future NEXRAD releases. The initial version of IHL currently provides the first icing detection algorithm for NEXRAD and future versions will enhance the algorithms ability to provide icing aviation hazard weather information for the FAA.

8. ACKNOWLEDGEMENTS

9. REFERENCES

Adriaansen, D. R., C. A. Wolff, and M. K. Politovich, 2012: Performance Analysis of the Current Icing Product (CIP) Algorithm under Variations in Icing Relevant Observational Datasets, *Proc. 4th AIAA Atmospheric and Space Environments Conference, 25-28 June 2012, New Orleans, Louisiana.*

American Meteorological Society, cited 2013: "snow pellets." Glossary of Meteorology. [Available online at http://glossary.ametsoc.org/wiki/Snow_pellets]

Bernstein, B. C., C. A. Wolff, and F. McDonough, 2007: An Inferred Climatology of Icing Conditions Aloft, Including Supercooled Large Drops. Part I: Canada and the Continental United States. *J. Appl. Meteor.*, **46,** 1857–1878.

Bernstein, B. C., F. McDonough, M. K. Politovich, B. G. Brown, T. P. Ratvasky, D. R. Miller, C. A. Wolff, and G. Cunning 2005: Current Icing Potential: Algorithm Description and Comparison with Aircraft Observations. *J. Appl. Meteor. Climatol.*, **44**, 969-986.

Elmore K. L., 2011: The NSSL Hydrometeor Classification Algorithm in Winter Surface Precipitation: Evaluation and Future Development, *Wea. Forecasting*, **26**, 756-765.

FAA, 2013a: US DOT-FAA Library – Flight Services, Chapter 9 (FAA Weather Services) Section 2: Pilot Weather Report.

FAA, 2013b: US DOT-FAA Library – Flight Services, Chapter 7 (Safety of Flight) .

Ganger, T., M. J. Istok, S. Shema, and B. Bumgarner, 2002: The WSR-88D Common Operations and Development Environment - Status and Future Plans, 18th Conf. On Interactive Information Processing Systems, January 2002, Orlando, FL.

Giangrade, S. E., J. M. Krause, and A. V. Ryzhkov, 2008: Automatic Designation of the Melting Layer with a Polarimetric Prototype of the WSR-88D Radar. *J. Appl. Meteor.*, **47**, 1354-1364.

Haggerty, J., F. M. McDonough, J. Black, G. Cunning, G. McCabe, M. Politovich, and C. Wolff, 2012: A System for Nowcasting Atmospheric Conditions Associated with Jet Engine Power Loss and Damage Due to Ingestion of Ice Particles, *Proc. 4th AIAA Atmospheric and Space Environments Conference, 25-28 June 2012, New Orleans, Louisiana.*

Heinselman, P.L. and A. V. Ryzhkov, 2006: Validation of Polarimetric Hail Detection. *Wea. Forecasting*, **21**, 839–850.

NTSB, 2013: Data query NTSB Aviation Accident Database.

Park, H. S., A. V. Ryzhkov, D. S. Zrnic, and Kyung-Eak Kim 2009: The Hydrometeor Classification Algorithm for the Polarimetric WSR-88D: Description and Application to an MCS. *Wea. Forecasting,* **24**, 730-748.

Smalley, D. J. and B. J. Bennett, 2002: Using ORPG to Enhance NEXRAD Products to Support FAA Critical Systems*. Proc. American Meteorological Society's 10th Conference on Aviation, Range, and Aerospace Meteorology, Portland, OR.*

Smalley, D. J., B. J. Bennett, M. F. Donovan, R. G. Hallowell, K. T. Hood, E. R. Williams, D. Zrnic, A. V. Ryzhkov, T. J. Schuur, H. D. Reeves, J. M. Krause, P. Zhang, M. Kumjian, J. Picca, S. Ganson, J. C. Hubbert, D. Albo, S. Ellis, M. Dixon, A. Weekley, M. Politovich, G. Cunning, C. Wolff, F. McDonough, T. Bals-Elsholz, R. Evaristo, and A. Stepanek, 2011: Multiple national laboratory and university partnership to develop dual polarization weather radar for the FAA. *Proc. American Meteorological Society's 27[h] Interactive Information Processing Systems Conference, Seattle, WA.*

Smalley, D. J., E. R. Williams, M. F. Donovan, R. G. Hallowell, K. T. Hood, B. J. Bennett, M. Wolde, M. Bastian, and A. Korolev, 2013: In Situ Icing Verification. *Proc. American Meteorological Society's 36th International Radar Conference, Breckenridge, CO.*

Williams, E. R., D. J. Smalley, M. F. Donovan, R. G. Hallowell, K. T. Hood, B. J. Bennett, R. Evaristo, A. Stepanek, T. Bals-Elsholz, J. Cobb, and J. M. Ritzman, 2011: Dual polarization radar winter storm studies supporting development of NEXRAD-based aviation hazard products. *Proc. American Meteorological Society's 35th International Radar Conference, Pittsburgh, PA.*

Wolff, C. A., M. K. Politovich, D. R. Adriaansen, A. F. Loughe, M. A. Petty, and J. L. Mahoney, 2012: Recent and Future Improvement in Automated Icing Algorithms, *Proc. 4th AIAA Atmospheric and Space Environments Conference, 25-28 June 2012, New Orleans, Louisiana.*